

Extracellular cholesterol-rich microdomains generated by human macrophages and their potential function in reverse cholesterol transport

Daniel S. Ong,^{*,†} Joshua J. Anzinger,^{*} Francisco J. Leyva,^{*} Noa Rubin,[§] Lia Addadi,[§] and Howard S. Kruth^{1,*}

Section of Experimental Atherosclerosis,^{*} National Heart, Lung, and Blood Institute, National Institutes of Health, Bethesda, MD 20892-1422; Clinical Research Training Program, National Institutes of Health, Bethesda, MD 20892; Department of Structural Biology,[§] Weizmann Institute of Science, 76100, Rehovot, Israel

Abstract Previous studies have shown that cholesterol in atherosclerotic plaques is present in both intracellular and extracellular forms. In the current study, we investigated a mechanism for extracellular cholesterol accumulation and examined the capacity of this pool of cholesterol to be removed by cholesterol acceptors, a step in reverse cholesterol transport. Human monocyte-derived macrophages differentiated with macrophage-colony stimulating factor were incubated with acetylated LDL to allow cholesterol enrichment and processing. These macrophages were subsequently labeled with a monoclonal antibody that specifically detects ordered cholesterol arrays, revealing the presence of unesterified cholesterol-rich microdomains on the cell surfaces and in the extracellular matrix. Similar unesterified cholesterol-rich microdomains were present in human atherosclerotic plaques. Actin microfilaments functioned in microdomain deposition or maintenance, and Src family kinases regulated transfer of these microdomains from the cell surface onto the extracellular matrix. Mediators of reverse cholesterol transport, apolipoprotein A-I (apoA-I), and HDL were capable of removing these extracellular unesterified cholesterol-rich microdomains. However, apoA-I removed the microdomains only when macrophages were present. ApoA-I removal of microdomains was blocked by glyburide and inhibitor of ATP-binding cassette transporter A1 (ABCA1) function. **In summary, cultures of cholesterol-enriched human monocyte-derived macrophages generate extracellular unesterified cholesterol-rich microdomains, which can subsequently be removed by cholesterol acceptors and therefore potentially function in reverse cholesterol transport.**—Ong, D. S., J. J. Anzinger, F. J. Leyva, N. Rubin, L. Addadi, and H. S. Kruth. **Extracellular cholesterol-rich microdomains generated by human macrophages and their potential function in reverse cholesterol transport.** *J. Lipid Res.* 2010. 51: 2303–2313.

Supplementary key words atherosclerosis • unesterified • macrophage-colony stimulating factor • Src family kinase • actin • apolipoprotein A-I • high-density lipoprotein

Atherosclerosis is the principle cause of coronary artery disease and stroke, and thus, understanding the mechanisms by which atherosclerotic plaques originate and progress is of great importance. Previous studies suggest that atherosclerotic plaques may develop as a result of an imbalance between cholesterol accumulation and cholesterol removal (1). The macrophage plays a central role in both of these processes (2–5), and, accordingly, the mechanisms behind the formation of lipid-laden macrophages termed “foam cells” (6) and reverse cholesterol transport mediated by these cells have been extensively studied. Atherosclerotic plaques, however, contain cholesterol in both intracellular and extracellular forms (7), and the etiology and fate of extracellular cholesterol in atherosclerosis is far less understood compared with intracellular cholesterol.

There is still much debate regarding the prominent pools of extracellular lipid that contribute to the necrotic core of advanced atherosclerotic lesions. The observations that large lipid pools are often found in relatively acellular areas and that excess cholesterol accumulation can be toxic to cells (8, 9) form the basis of the prevailing theory that the necrotic core forms as macrophages die and release their accumulated cholesterol into the extracellular space (10). Chemical analyses, however, have shown that extracellular lipid particles isolated from atherosclerotic regions of human aortas are more similar in composition

This research was made possible through the Clinical Research Training Program, a public-private partnership supported jointly by the National Institutes of Health and Pfizer Inc (via a grant to the Foundation for the National Institutes of Health from Pfizer Inc). Its contents are solely the responsibility of the authors and do not necessarily represent the official views of the National Institutes of Health or other granting agencies.

Manuscript received 22 January 2010 and in revised form 26 April 2010.

Published, JLR Papers in Press, April 26, 2010

DOI 10.1194/jlr.M005660

Abbreviations: ABCA1, ATP-binding cassette transporter A1; ACAT, Acyl-CoA:cholesterol acyltransferase; AcLDL, acetylated LDL; apoA-I, apolipoprotein A-I; DAPI, 4'-6-Diamidino-2-phenylindole; DPBS, Dulbecco's phosphate-buffered saline; GM-CSF, granulocyte macrophage-colony stimulating factor; IL-10, interleukin-10; MAb, monoclonal antibody; M-CSF, macrophage-colony stimulating factor.

¹To whom correspondence should be addressed.
e-mail: kruthh@nhlbi.nih.gov

to plasma lipoproteins than they are to cellular lipid droplets (11), suggesting that extracellular lipid is not simply the released contents of dying macrophages. Data from these studies contribute to an alternative theory that extracellular cholesterol is a product of LDL that has been deposited within the extracellular matrix, taken up by cells, processed, and resecreted in the form of liposomes enriched in unesterified cholesterol (12). It may be that both of these theories are correct and that multiple mechanisms contribute to the accumulation of extracellular cholesterol, underscoring the complexity of cholesterol deposition in atherosclerosis.

In this study, we sought to further investigate the theory that the extracellular lipid particles found in atherosclerotic lesions represent plasma lipoprotein that has been taken up by macrophages, processed, and effluxed. Unesterified cholesterol has previously been detected in atherosclerotic lesions using filipin, a fluorescent polyene antibiotic that binds to the 3β -hydroxyl unit of single unesterified cholesterol molecules (13). Because cholesterol is ubiquitously present in cell membranes, filipin cannot distinguish between the pool of cholesterol found in all cells, that which may be uniquely involved in reverse cholesterol transport or that which may represent pathologic accumulation. To address this difficulty, we utilized a monoclonal antibody (MAb), 58B1, raised against cholesterol monohydrate crystals. This antibody has previously been reported to label ordered arrays of approximately 12 molecules of unesterified cholesterol without recognizing individual cholesterol molecules (14, 15) and has been successfully used to label cell surface microdomains of unesterified cholesterol in human monocyte-derived macrophages differentiated using human serum. These macrophages are similar to monocyte-derived macrophages differentiated with FBS with added granulocyte macrophage-colony stimulating factor (GM-CSF) (16). Previous studies have shown that monocytes differentiated using FBS with added macrophage-colony stimulating factor (M-CSF) produce macrophages in culture that are more similar in shape and cell surface marker expression to those that predominate in atherosclerotic lesions than monocytes differentiated using FBS with added GM-CSF (16). We therefore conducted our experiments using cultures of these M-CSF-differentiated human monocyte-derived macrophages to more closely model cholesterol processing in vivo. Using these experimental tools, we tested the hypothesis that cholesterol-enriched macrophages produce extracellular accumulations of unesterified cholesterol and also examined whether cholesterol acceptors can remove this pool of cholesterol, a step in reverse cholesterol transport.

MATERIALS AND METHODS

Materials

RPMI 1640 was obtained from Mediatech (Herndon, VA); FBS and Dulbecco's phosphate-buffered saline with Ca^{2+} and Mg^{2+} (DPBS) were obtained from Invitrogen (Carlsbad, CA); 12-well CellBIND plates were obtained from Corning (Corning,

NY); M-CSF and interleukin-10 (IL-10) were obtained from PeproTech (Rocky Hill, NJ); acetylated LDL (AcLDL) and HDL were obtained from Intracel (Frederick, MD); cytochalasin D and SU6656 were obtained from Calbiochem (La Jolla, CA); apolipoprotein A-I (apoA-I) was obtained from Chemicon (Charlottesville, VA); BSA and OCT embedding media were obtained from Electron Microscopy Sciences (Hatfield, PA); SuperFrost Plus slides were obtained from Menzel Glazer; oil-red O, isopropyl alcohol, Mayer's hematoxylin, glycerol gelatin, nocodazole, and glyburide were obtained from Sigma (St. Louis, MO); paraformaldehyde was obtained from Polysciences (Warrington, PA); FcR Blocking Reagent (human) was obtained from Miltenyi Biotec (Auburn, CA); mouse anti-cholesterol array MAb 58B1 IgM in ascites was produced as previously described (14); mouse anti-*Clavibacter michiganense* MAb (clone 9A1) IgM in ascites was obtained from Agdia (Elkhart, IN); and avidin/biotin blocking kit, biotinylated goat anti-mouse IgM, fluorescein-avidin and Vectashield hard set mounting medium with 4'-6-Diamidino-2-phenylindole (DAPI) were obtained from Vector Laboratories (Burlingame, CA).

Culture of human monocyte-derived macrophages

Mononuclear cells were obtained from human donors by monocytopheresis and subsequently purified using counterflow centrifugal elutriation as previously described (17). Monocytopheresis was carried out under a human subjects research protocol approved by a National Institutes of Health institutional review board. A different human donor was used for each experiment. The resulting elutriated human monocytes were diluted in RPMI 1640 medium containing 10% FBS and seeded onto 12-well CellBIND plates at a density of 2×10^5 cells/cm². Cultures were incubated in a 37°C cell culture incubator with 5% CO₂/95% air for 2 h and subsequently rinsed three times with RPMI 1640 to remove nonadherent cells. The remaining adherent cells were then differentiated with 50 ng/ml M-CSF and 25 ng/ml IL-10 in RPMI 1640 (hereafter referred to as "media") plus 10% FBS. IL-10 was included because it enhances the growth and differentiation of human monocytes cultured in M-CSF and creates a more homogenous macrophage phenotype (18). Cultures were washed and replaced with fresh media on day 6. The resulting monocyte-derived macrophages were used for experiments on day 7.

Immunostaining of cultured human monocyte-derived macrophages

Fixation, immunostaining, and microscopy were all performed with macrophages in their original CellBIND culture plates, and all steps were carried out at room temperature. One-week-old monocyte-derived macrophage cultures were rinsed three times in DPBS, fixed for 10 min with 4% paraformaldehyde in DPBS, and then rinsed an additional three times in DPBS. Cells were then incubated 60 min with 5 $\mu\text{g}/\text{ml}$ mouse anti-cholesterol microdomain MAb 58B1 IgM diluted in DPBS containing 0.1% BSA. Control staining was performed with an irrelevant purified mouse anti-*Clavibacter michiganense* MAb (clone 9A1) IgM diluted in DPBS containing 0.1% BSA. Cultures were then rinsed three times (5 min each) in DPBS, followed by a 30-min incubation in 5 $\mu\text{g}/\text{ml}$ biotinylated goat anti-mouse IgM diluted in DPBS containing 0.1% BSA. After three rinses in DPBS (5 min each), cultures were incubated 30 min with 20 $\mu\text{g}/\text{ml}$ fluorescein-avidin in 0.1 M sodium bicarbonate buffer with 0.15 M NaCl added (final pH 8.2). Cultures were then rinsed three times with DPBS and mounted in Vectashield mounting medium with DAPI nuclear stain in preparation for digital imaging using an Olympus IX81 fluorescence microscope.

Microscopic analysis

Cells were identified using phase contrast microscopy or by locating DAPI-stained nuclei. The pattern and intensity of MAb 58B1 staining were then analyzed for cultures from each experimental parameter, and these data were compared with one another. MAb 58B1-labeling was considered cellular if it was located within cell membrane boundaries, as identified on the corresponding phase contrast view. Labeling was considered extracellular if it was located outside the cell membrane boundaries seen on phase contrast view. Different planes of focus were visualized before acquiring images to confirm that only a monolayer of cells was present, thereby ensuring that labeling seen outside cell membrane boundaries did not represent cellular labeling from cells lying in a different plane of focus.

Quantification of cholesterol from macrophages

After incubations, human monocyte-derived macrophage cultures were rinsed three times in DPBS. Macrophages were then harvested from wells by scraping into 1 ml distilled water. Lipid was extracted from the resulting cell suspension using the Folch method (19), and quantities of esterified and unesterified cholesterol were determined using the method previously described by Gamble et al. (20). Protein quantification was performed on an aliquot of cell lysate using the Lowry method (21) with BSA as a standard. Data are represented as means \pm SEM. Means were determined from three culture wells for each data point, and statistical comparisons of means were made using the Student's *t*-test (unpaired). A *P*-value of ≤ 0.05 was considered significant.

Staining of human aortic tissue sections

Human aortic tissue was obtained from autopsy of a 49-year-old individual who died of myocardial infarction (National Disease Research Interchange, Philadelphia, PA). The aortic tissue was snap frozen in liquid nitrogen and embedded in OCT media. Then 10 μ m frozen sections were prepared from regions with and without lipid deposits visible on gross inspection, placed onto gelatin-coated slides (SuperFrost Plus), and then stored at -80°C until further processing.

For oil-red O staining, frozen tissue sections were thawed at room temperature and rehydrated with distilled water. Sections were fixed for 10 min with 1.6% paraformaldehyde in DPBS followed by a single rinse in DPBS. Samples were then treated with 60% isopropyl alcohol for 2 min, stained for 20 min with 0.5% oil-red O, followed by an additional treatment with 60% isopropyl alcohol for 1 min. Sections were washed twice with distilled water and then treated with Mayer's hematoxylin for 5 min to stain nuclei blue. Following a 5 min rinse in distilled water, sections were mounted in glycerol-gelatin in preparation for imaging. All steps were carried out at room temperature.

For fluorescence immunostaining, separate frozen tissue sections adjacent to sections stained with oil-red-O were thawed at room temperature and rehydrated with distilled water. Sections were then fixed for 30 min with 4% paraformaldehyde in DPBS. After three rinses in DPBS, sections were blocked for 10 min with human FcR blocking reagent and for 15 min with avidin and biotin blocking solutions. Sections were then immunostained using the mouse anti-cholesterol array IgM MAb 58B1 or the irrelevant control antibody, purified mouse anti-*Clavibacter michiganense* IgM MAb (clone 9A1), according to the protocol described above for cultured human monocyte-derived macrophages. All steps were carried out at room temperature, and digital imaging was performed using an Olympus IX81 fluorescence microscope.

RESULTS

Antibody labeling of extracellular unesterified cholesterol-rich microdomains in cell culture

We incubated macrophage cell cultures with AcLDL (50 $\mu\text{g}/\text{ml}$) for 1 day to enrich them with cholesterol. Serum was not included in the culture media at this point to prevent the introduction of potential cholesterol acceptors to our experimental system. Generation of extracellular unesterified cholesterol-rich microdomains was then confirmed using MAb 58B1. Fluorescence microscopy revealed antibody labeling of unesterified cholesterol-rich microdomains on macrophage cell surfaces as well as in the extracellular spaces between cells (arrows in Fig. 1A, B). The extracellular unesterified cholesterol-rich microdomains appeared as spherical microparticles. The unesterified cholesterol-rich microdomains did not represent AcLDL that had simply adhered to the culture plate, as slides coated with AcLDL did not label with MAb 58B1. Cultures incubated with AcLDL for 2 days (Fig. 1B) produced more extracellular unesterified cholesterol-rich microdomain labeling than cultures incubated for only 1 day (Fig. 1A), suggesting that the generation of these micro-

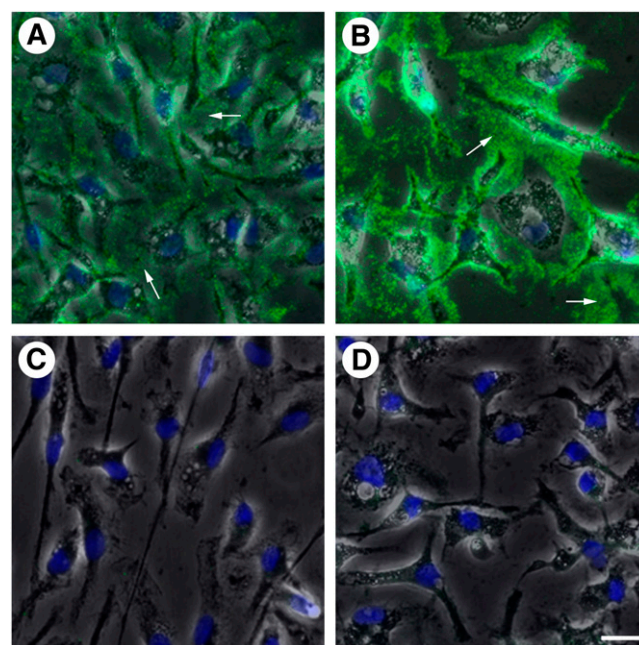


Fig. 1. Incubation of human monocyte-derived macrophage cultures with AcLDL results in the generation of extracellular unesterified cholesterol-rich microdomains. Human monocyte-derived macrophages differentiated in the presence of M-CSF for 1 week were incubated with AcLDL (50 $\mu\text{g}/\text{ml}$) for 1 (A) or 2 days (B) or without AcLDL for 1 day (C). Staining with the anti-unesterified cholesterol array MAb 58B1 (green in A–C) revealed extracellular unesterified cholesterol-rich microdomains (arrows) in cultures incubated with AcLDL but not in cultures incubated without AcLDL. Cells were visualized using phase contrast microscopy (gray) and nuclei were stained using DAPI (blue). Control staining using an irrelevant Mab anti-*Clavibacter michiganense* clone 9A1 (green in D), following 1 day incubation with AcLDL revealed no staining. Bar = 25 μm and applies to all.

domains occurs continuously from cholesterol-enriched macrophages. Labeling with MAb 58B1 was not detected in cultures incubated without AcLDL (Fig. 1C), and cultures incubated with AcLDL but stained with an irrelevant purified mouse anti-*Clavibacter michiganense* antibody (MAb clone 9A1) similarly did not produce observable labeling (Fig. 1D).

Antibody labeling of unesterified cholesterol-rich microdomains in human aortic tissue sections

We next sought to determine if the extracellular unesterified cholesterol-rich microdomains identified in cholesterol-enriched macrophage cultures are also present in vivo. Aortic tissue sections were obtained from the autopsy specimen of an individual who died of myocardial infarction, and adjacent sections from various regions of the aorta were stained with oil-red O, which labels esterified cholesterol-containing oil-phase lipid droplets, or MAb 58B1, which labels only unesterified cholesterol. The resulting patterns of labeling were compared to determine if there was a correlation between the prevalence of lipid-enriched cells such as macrophage foam cells, as evidenced by staining with oil-red O, and the distribution of unesterified cholesterol-rich microdomains, as evidenced by staining with MAb 58B1. Consistent with our hypothesis that foam cells produce these microdomains, regions that contained oil-red O-labeled foam cells also labeled with the anti-cholesterol microdomain antibody (Fig. 2A, B), whereas regions that lacked oil-red O-labeled foam cells (but showed only fine extracellular oil-red O staining previously attributed to extracellular deposits of LDL) (22) also lacked unesterified cholesterol-rich microdomains (Fig. 2C, D).

Function of cytoskeleton in generation of extracellular unesterified cholesterol-rich microdomains

We next sought to manipulate the cell cytoskeleton to determine if doing so would interfere with the production of extracellular unesterified cholesterol-rich microdomains. Cytochalasin D has been shown to inhibit actin polymerization, thereby disrupting the microfilament cytoskeleton (23). We incubated human monocyte-derived macrophage cultures with AcLDL (50 $\mu\text{g}/\text{ml}$) for 1 day to allow cholesterol enrichment and processing. Cultures were then washed and incubated for a second day with media alone or media plus 4 $\mu\text{g}/\text{ml}$ cytochalasin D and then stained with MAb 58B1 to visualize unesterified cholesterol-rich microdomains. In cultures incubated with AcLDL followed by media alone, punctate labeling was visualized in the extracellular space, confirming the presence of extracellular unesterified cholesterol-rich microdomains (Fig. 3A, B). In contrast, cultures incubated with AcLDL followed by media plus cytochalasin D produced no labeling when stained with MAb 58B1 (Fig. 3C, D). This finding suggests an important function for actin microfilaments in either the deposition or maintenance of unesterified cholesterol-rich microdomains in the extracellular matrix.

We similarly studied the effect of nocodazole, an inhibitor of microtubule formation (24), on the deposition of extracellular unesterified cholesterol-rich microdomains.

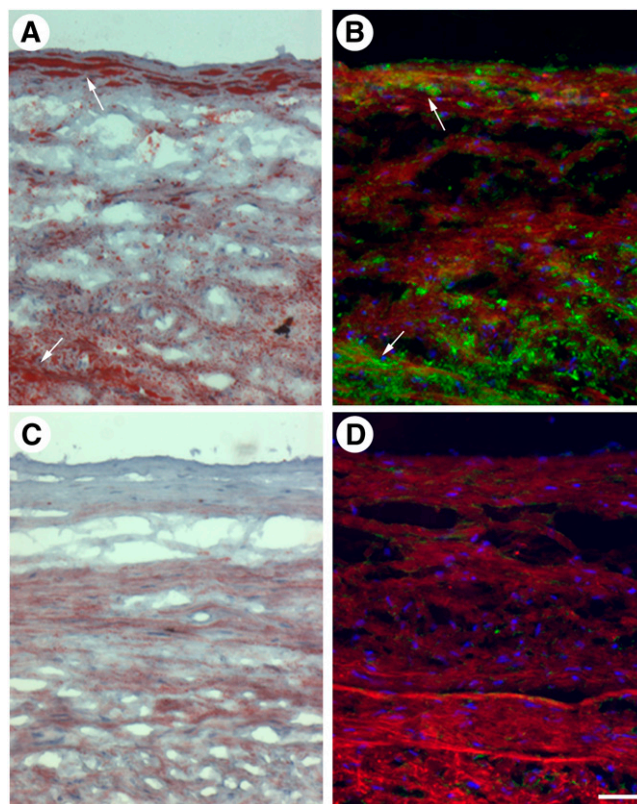


Fig. 2. Unesterified cholesterol-rich microdomains are found in regions of human aortic tissue with lipid-containing foam cells. Regions of human aortic tissue with (arrows in A and B) and without (C and D) lipid-rich foam cells were identified by oil-red O staining (red in A and C), and adjacent tissue sections were labeled with MAb 58B1 (green in B and D). Cell nuclei were stained using either hematoxylin (blue in A and C) or DAPI (blue in B and D), and tissue autofluorescence (red in B and D) was used to visualize vessel structure. Bar = 85 μm and applies to all.

Cultures incubated for 1 day with 50 $\mu\text{g}/\text{ml}$ AcLDL followed by incubation for a second day in media with 5 μM nocodazole were stained with MAb 58B1. We observed that treatment with nocodazole, in contrast to treatment with cytochalasin D, did not reduce extracellular unesterified cholesterol-rich microdomain labeling (Fig. 3E, F). Thus, microtubules do not contribute to the deposition of these microdomains onto the extracellular matrix.

Function of Src family kinase signaling pathway in generation of extracellular unesterified cholesterol-rich microdomains

Members of the Src family of tyrosine kinases have been shown to function in the regulation of the actin cytoskeleton (25–27), and at least six are expressed in human monocyte-derived macrophages (28). We therefore hypothesized that the Src family kinase-signaling cascade could be involved in the regulation of extracellular unesterified cholesterol deposition. SU6656 is a compound that has been shown to inhibit Src family kinase activity (29). Human monocyte-derived macrophage cultures were pretreated without or with 20 μM SU6656 for 1 h. Cultures were then incubated for 2 days with 50 $\mu\text{g}/\text{ml}$ AcLDL without or with 20 μM SU6656, depending on the pretreatment condition,

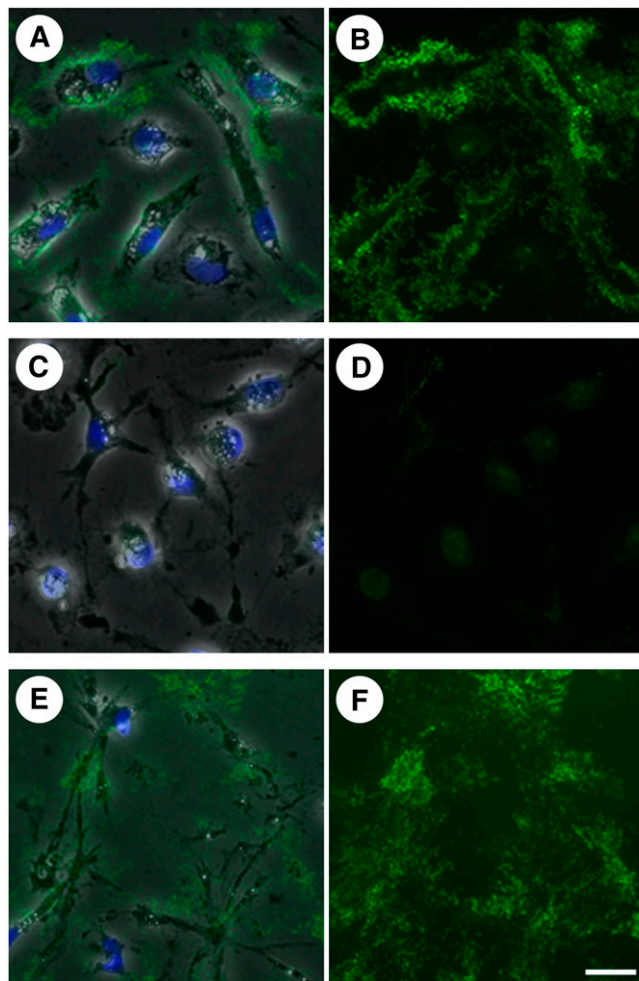


Fig. 3. Actin microfilaments are involved in the deposition or retention of unesterified cholesterol-rich microdomains in the extracellular matrix. One-week-old macrophage cultures were incubated for 1 day with AcLDL (50 $\mu\text{g}/\text{ml}$), followed by incubation for a second day in media with no addition (A and B), media plus 4 $\mu\text{g}/\text{ml}$ cytochalasin D to inhibit actin polymerization (C and D), or media plus 5 μM nocodazole to inhibit microtubule formation (E and F). Unesterified cholesterol-rich microdomains were labeled with MAb 58B1 (green), and cells were visualized using phase contrast microscopy (gray) and DAPI nuclear stain (blue). Images are also shown with MAb 58B1 staining alone (B, D, and F) for clarity. Bar = 25 μm and applies to all.

and subsequently stained with MAb 58B1. Cultures incubated without SU6656 demonstrated labeling of unesterified cholesterol-rich microdomains on cell surfaces and in the extracellular matrix (Fig. 4A–C), consistent with results above. Cultures incubated with SU6656, however, showed no extracellular labeling with MAb 58B1 and a concomitant increase in cell surface labeling (Fig. 4D–F) when compared with cultures incubated without SU6656.

To ensure that these results reflect a regulatory function for Src family kinases in cholesterol processing rather than cholesterol uptake, we performed a quantification assay to determine if SU6656 affects cholesterol enrichment. At baseline, human monocyte-derived macrophage cultures contained an average of 83 ± 0 (mean \pm SEM) nmol cholesterol/mg protein. Cultures were then pretreated for 1 h

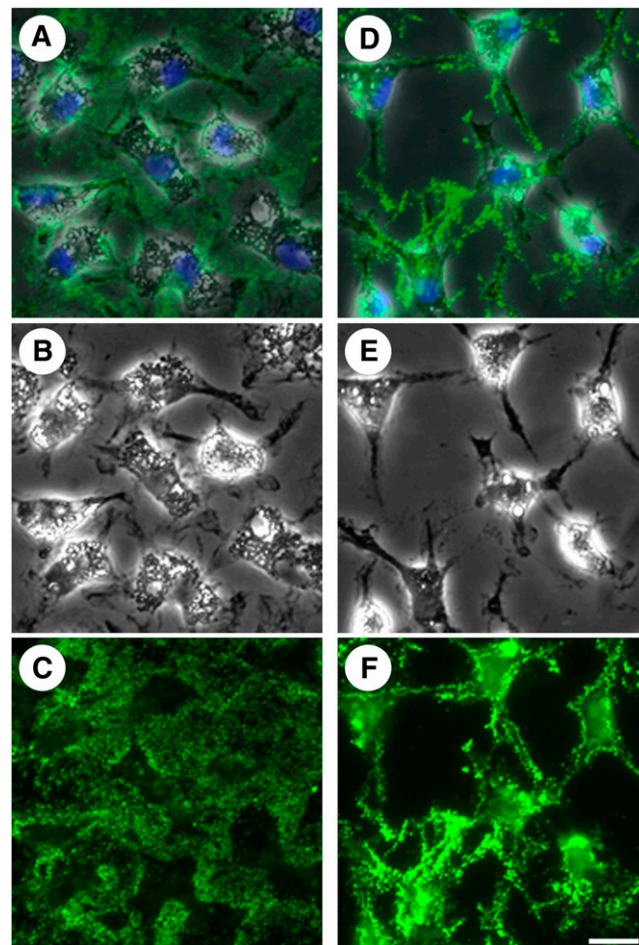


Fig. 4. Inhibition of Src family kinase activity interferes with transfer of unesterified cholesterol from cell surface onto extracellular matrix. One-week-old macrophage cultures were incubated with AcLDL (50 $\mu\text{g}/\text{ml}$) alone (A–C) or plus the Src family kinase inhibitor, SU6656 (20 μM) (D–F) for 2 days. Cultures were stained with MAb 58B1 (green), and cells were visualized using phase contrast microscopy (gray) and DAPI nuclear stain (blue). Phase contrast images (B and E) and unesterified cholesterol-rich microdomain staining (C and F) are also shown separately for each condition for clarity. Bar = 25 μm and applies to all.

without or with 20 μM SU6656 and then incubated for 24 h with 25 $\mu\text{g}/\text{ml}$ AcLDL without or with 20 μM SU6656 depending on the pretreatment condition. Total cholesterol content in both treatment groups increased significantly above baseline ($P = 0.003$) but did not differ significantly between treatment conditions; cultures incubated with AcLDL alone contained an average of 279 ± 12 (mean \pm SEM) nmol cholesterol/mg protein compared with cultures incubated with AcLDL and SU6656, which contained 305 ± 12 nmol/mg protein ($P = 0.193$) (Fig. 5).

Extracellular unesterified cholesterol-rich microdomains can function in reverse cholesterol transport

Although we have shown that cholesterol-enriched macrophages can generate extracellular unesterified cholesterol-rich microdomains, the function of these microdomains remains unclear. It has previously been suggested that extracellular accumulations of unesterified

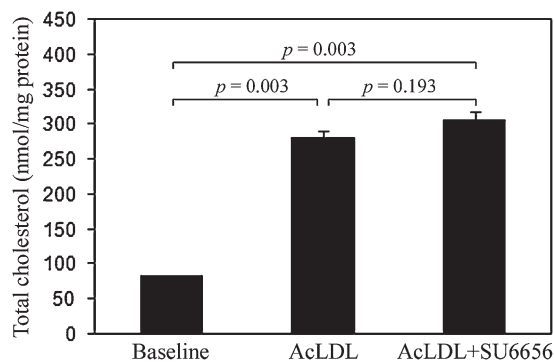


Fig. 5. Inhibition of Src family kinase activity does not alter total cholesterol uptake. One-week-old macrophage cultures were pretreated without and with the Src family kinase inhibitor, SU6656 (20 μ M), for 1 h and subsequently incubated with AcLDL (50 μ g/ml) alone or plus SU6656 (20 μ M) for 2 days. Quantities of total cholesterol were determined, and the results are plotted as the mean \pm SEM of triplicate cultures. Statistical significance ($P \leq 0.05$) was determined using the Student's *t*-test (unpaired).

cholesterol-rich microdomains may be constituents of a reverse cholesterol transport pathway (12). We therefore hypothesized that the microdomains identified using MAb 58B1 are capable of being removed by HDL and apoA-I, cholesterol acceptors known to function in reverse cholesterol transport. ApoA-I is an indirect cholesterol acceptor in that it mobilizes cholesterol only after the apoA-I complexes with phospholipid, the agent that binds cholesterol both in phospholipidated apoA-I and HDL (30, 31). Human monocyte-derived macrophage cultures were incubated with 50 μ g/ml AcLDL for 1 day to allow cholesterol enrichment and generation of extracellular microdomains. Cultures were then washed and incubated in media without or with a cholesterol acceptor (HDL or apoA-I at 50 μ g/ml) for a second day. Additionally, these results were compared with cultures incubated without AcLDL on the first day and without a cholesterol acceptor on the second day, which produced no labeling when stained with MAb 58B1 (Fig. 6A, B). Cholesterol-enriched macrophage cultures that were not treated with a cholesterol acceptor-produced cell surface and extracellular microdomain labeling with MAb 58B1 (Fig. 6C, D), consistent with results presented above. In contrast, cholesterol-enriched macrophages that were treated with the cholesterol acceptors, HDL (Fig. 6E, F) or apoA-I (Fig. 6G, H), showed reduced or no labeling with MAb 58B1 both on cell surfaces and in the extracellular matrix, suggesting that these cholesterol acceptors can indeed remove these unesterified cholesterol-rich microdomains. We also observed that treatment of cholesterol-enriched macrophages with BSA did not reduce MAb 58B1-labeling (data not shown). This supports the idea that the capacity to remove these unesterified cholesterol-rich microdomains is a feature unique to known mediators of the reverse cholesterol transport system.

To evaluate the efficacy of cholesterol removal in this system, we also performed a cholesterol quantification assay on cultures processed in the same conditions as described above (Fig. 6, graph). Cultures that received no

AcLDL on the first day and no cholesterol acceptor on the second day contained an average of 78 ± 2 nmol unesterified cholesterol and 2 ± 1 nmol esterified cholesterol/mg protein. Incubation with AcLDL for 1 day produced cultures with an average of 285 ± 11 nmol unesterified cholesterol and 178 ± 8 nmol esterified cholesterol/mg protein, indicating that cholesterol enrichment results in the average net accumulation of 207 nmol unesterified cholesterol and 176 nmol esterified cholesterol/mg protein. Treatment with HDL reduced unesterified cholesterol content by 34% ($P = 0.001$) to 188 ± 6 nmol/mg protein, whereas esterified cholesterol levels remained unchanged at 176 ± 6 nmol/mg protein ($P = 0.825$). Similarly, treatment with apoA-I reduced unesterified cholesterol by 42% ($P = 0.002$) to 165 ± 11 nmol/mg protein, but esterified cholesterol levels remained unchanged at 153 ± 10 nmol/mg protein ($P = 0.116$). Although the cholesterol quantification assay cannot distinguish between unesterified cholesterol within cells, on the cell surface, or in the extracellular matrix, this data is consistent with the results of the MAb 58B1 immunostaining showing that unesterified cholesterol-rich microdomains can be removed by the cholesterol acceptors, HDL and apoA-I.

Removal of extracellular unesterified cholesterol microdomains by apoA-I requires the presence of cells whereas removal by HDL does not

We next sought to determine if the removal of unesterified cholesterol-rich microdomains from the extracellular space requires cellular function. Human monocyte-derived macrophage cultures were incubated with 50 μ g/ml AcLDL for 1 day and then subjected to three freeze-thaw cycles ($-80^{\circ}\text{C}/37^{\circ}\text{C}$) to lyse and remove cells. The extracellular matrix left behind was then incubated with or without a cholesterol acceptor (apoA-I or HDL at 50 μ g/ml) for a second day and stained with MAb 58B1. Removal of cells was confirmed using phase contrast microscopy.

Cholesterol-enriched cultures that were freeze-thawed and then incubated without a cholesterol acceptor (Fig. 7A, B) or with apoA-I (Fig. 7C, D) retained extracellular microdomain labeling, confirming that the freeze-thaw procedure in and of itself does not eliminate these microdomains and also showing that apoA-I requires the presence of cells to mediate removal of extracellular unesterified cholesterol-rich microdomains. In contrast, cholesterol-enriched cultures that were freeze-thawed and then treated with HDL produced no labeling when stained with MAb 58B1 (Fig. 7E, F). These results suggest that HDL, but not apoA-I, can remove extracellular unesterified cholesterol-rich microdomains in the absence of cells.

Removal of extracellular unesterified cholesterol-rich microdomains by apoA-I is inhibited by glyburide

Previous studies have shown that apoA-I must be phospholipidated through the action of the ATP-binding cassette protein, ABCA1, before it can act as a cholesterol acceptor (32). We therefore employed glyburide, an inhibitor of ABCA1 (32), to determine if the requirement of cells for apoA-I mediated removal of extracellular unesterified cholesterol-rich microdomains can be attributed

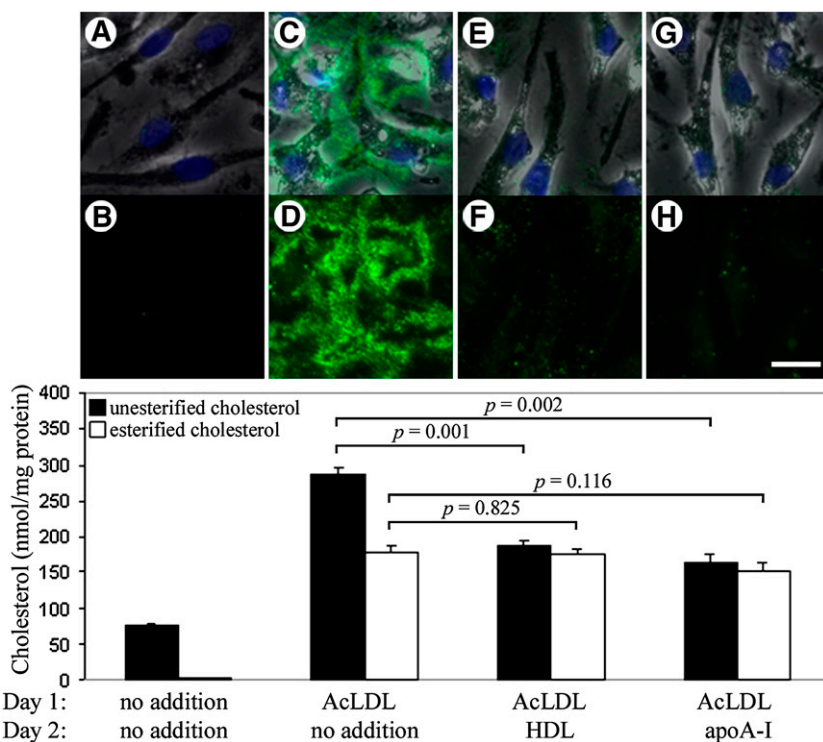


Fig. 6. Unesterified cholesterol-rich microdomains can be removed by cholesterol acceptors. One-week-old macrophage cultures were incubated with media alone for 2 days (A and B) or incubated for 1 day with AcLDL (50 $\mu\text{g}/\text{ml}$) followed by incubation for a second day with media alone (C and D), media plus 50 $\mu\text{g}/\text{ml}$ HDL (E and F), or media plus 50 $\mu\text{g}/\text{ml}$ apoA-I (G and H). Cultures were stained for unesterified cholesterol-rich microdomains using MAb 58B1 (green), and cells were visualized using phase contrast microscopy (gray) and DAPI nuclear stain (blue). Images are also shown with MAb 58B1 staining alone (B, D, F, and H) for clarity. Bar = 25 μm and applies to all. Quantities of unesterified and esterified cholesterol were also determined, and the results are plotted as the mean \pm SEM of triplicate cultures (graph). Statistical significance ($P \leq 0.05$) was determined using the Student's *t*-test (unpaired).

to the need for phospholipidation by ABCA1 or if other cell functions are also necessary. Human monocyte-derived macrophage cultures were incubated with 50 $\mu\text{g}/\text{ml}$ AcLDL for 1 day to allow cholesterol enrichment and deposition of extracellular cholesterol-rich microdomains. Cultures were then washed and pretreated in media with glyburide (100 μM) for 30 min followed by incubation for a second day with 100 μM glyburide alone or 50 $\mu\text{g}/\text{ml}$ apoA-I plus 100 μM glyburide. A third set of cultures was pretreated for 30 min in media without glyburide and subsequently incubated for a second day with 50 $\mu\text{g}/\text{ml}$ apoA-I alone. Cells were then stained with MAb 58B1 to determine the effect of glyburide on the capacity of apoA-I to remove extracellular unesterified cholesterol-rich microdomains. As shown above, no extracellular cholesterol-rich microdomain labeling was observed in cultures that received apoA-I alone (Fig. 8A, B). In contrast, cultures that received glyburide alone maintained extracellular unesterified cholesterol labeling (Fig. 8C, D), confirming that glyburide itself does not eliminate these microdomains. Cholesterol-enriched cultures treated with both apoA-I and glyburide (Fig. 8E, F) produced a MAb 58B1 labeling pattern and intensity that resembled cultures receiving glyburide alone. This result suggests that apoA-I mediated removal of extracellular microdomains is dependent on ABCA1 function, consistent with the known

mechanism for ApoA-I mediated removal of unesterified cholesterol from cell surfaces.

DISCUSSION

In this study, we confirmed our hypothesis that human monocyte-derived macrophages differentiated in the presence of M-CSF generate extracellular unesterified cholesterol-rich microdomains when incubated with AcLDL. These microdomains were identified using a Mab that labels ordered arrays of unesterified cholesterol, MAb 58B1, and were capable of being removed by cholesterol acceptors known to function in reverse cholesterol transport.

In a previous study, experiments using MAb 58B1 were conducted using cholesterol-enriched cultures of monocyte-derived macrophages differentiated with human serum (15). These macrophages have a rounded "fried-egg" appearance and require inhibition of Acyl-CoA:cholesterol acyltransferase (ACAT), which blocks esterification of cellular cholesterol, to induce the formation of plasma membrane unesterified cholesterol-rich microdomains that could be visualized using the antibody. Although extracellular unesterified cholesterol-rich microdomains were visualized in this earlier study, these extracellular domains were observed in association with only 10–20% of macrophages and depended on inhibition of ACAT activity

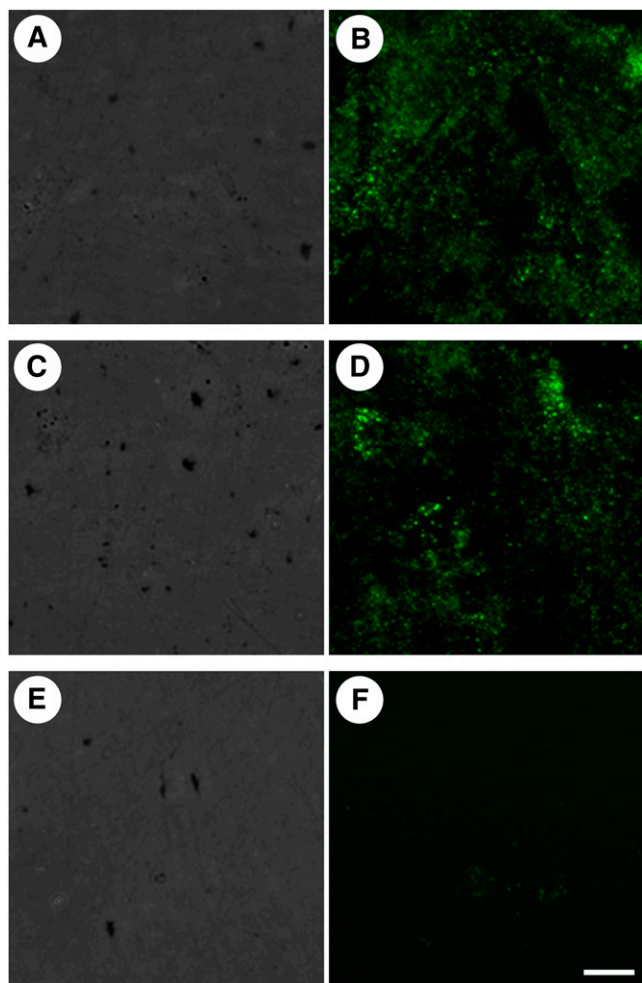


Fig. 7. Removal of extracellular unesterified cholesterol-rich microdomains by apoA-I depends on the presence of cells, whereas removal by HDL does not. One-week-old macrophage cultures were incubated with AcLDL (50 $\mu\text{g}/\text{ml}$) for 1 day to allow generation of extracellular unesterified cholesterol-rich microdomains. Cultures were then subjected to three freeze-thaw cycles to lyse and remove cells, and the remaining extracellular matrix was incubated for 1 day with media alone (A and B), media with 50 $\mu\text{g}/\text{ml}$ apoA-I (C and D), or media with 50 $\mu\text{g}/\text{ml}$ HDL (E and F). Cultures were imaged using phase contrast microscopy (A, C, and E) to confirm removal of cells, and extracellular unesterified cholesterol-rich microdomains were labeled with MAb 58B1 (B, D, and F). Bar = 25 μm and applies to all.

(15). In the current study, we used cholesterol-enriched human monocyte-derived macrophages cultures differentiated in the presence of M-CSF and were able to visualize MAb 58B1-labeled cell surface and extracellular cholesterol-rich microdomains in association with almost all macrophages, without the need for ACAT inhibition. This may have been because the M-CSF-differentiated macrophages accumulated substantially more unesterified cholesterol compared with the human serum-differentiated macrophages.

Because we found that these unesterified cholesterol-rich microdomains could be removed by mediators of the reverse cholesterol transport system, the cholesterol-processing pathway utilized by M-CSF-differentiated

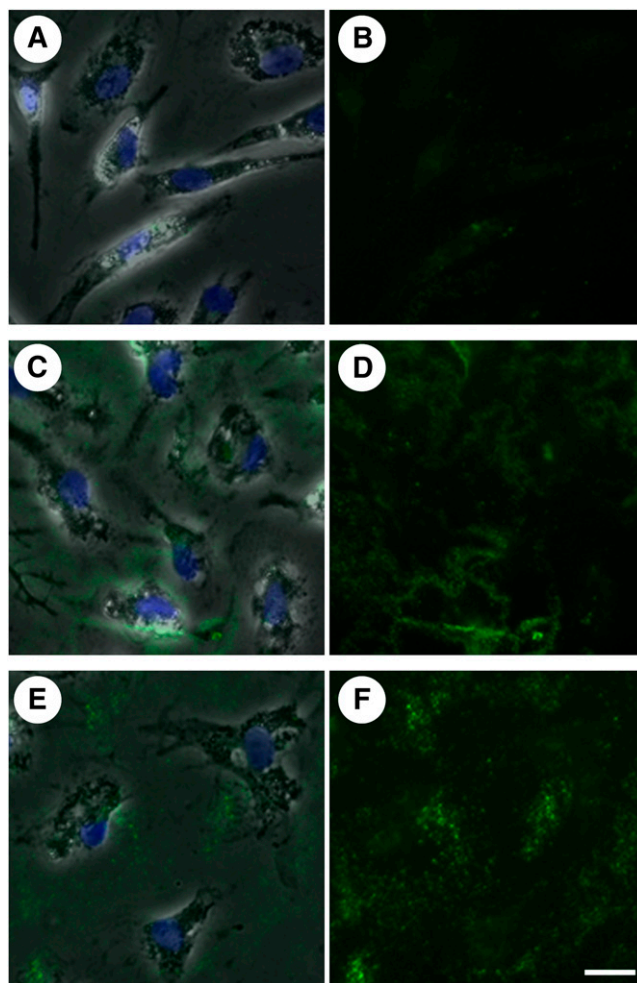


Fig. 8. ApoA-I mediated removal of extracellular unesterified cholesterol-rich microdomains is blocked by the ABCA1 inhibitor glyburide. One-week-old macrophage cultures were incubated with AcLDL (50 $\mu\text{g}/\text{ml}$) for 1 day to allow generation of extracellular unesterified cholesterol-rich microdomains. Cultures were then pretreated for 30 min without or with glyburide (100 μM) to inhibit ABCA1 function before incubation for a second day with 50 $\mu\text{g}/\text{ml}$ apoA-I (A and B), 100 μM glyburide (C and D), or both apoA-I and glyburide (E and F). Unesterified cholesterol-rich microdomains were labeled with MAb 58B1 (green), and cells were visualized using phase contrast microscopy (gray) and DAPI nuclear stain (blue). Images are also shown with MAb 58B1 staining alone (B, D, and F) for clarity. Bar = 25 μm and applies to all.

macrophages may represent an important pathway for cholesterol efflux. Because M-CSF-differentiated macrophages share a similar elongated phenotype and cell surface marker expression pattern to a subtype of macrophages found to predominate in atherosclerotic lesions (16), the cholesterol efflux pathway studied here may be the same pathway utilized by macrophage foam cells in atherosclerotic lesions in vivo. Consistent with this idea, we observed that regions of human aortic tissue that were identified by oil-red O staining to be enriched with cholesterol-enriched cells such as macrophage foam cells were also enriched with unesterified cholesterol-rich microdomains that labeled with MAb 58B1. On the other hand, regions of aortic tissue that were relatively devoid of dis-

ease and foam cells showed only minimal labeling with MAb 58B1.

Actin microfilaments were found to be necessary to maintain unesterified cholesterol-rich microdomains in the extracellular matrix. Because extracellular staining with MAb 58B1 is observed in cell cultures incubated with AcLDL for 1 day, we did not anticipate the complete lack of extracellular microdomain labeling observed in cultures incubated with AcLDL for 1 day followed by treatment with cytochalasin D to disrupt actin polymerization. One potential explanation for this finding is that the unesterified cholesterol-rich microdomains deposited by cells are constantly fluxing through the extracellular matrix such that individual cholesterol-rich microdomains are only transiently located in the matrix. In this scenario, macrophages must continuously deposit cholesterol-rich microdomains onto the extracellular matrix for them to accumulate and label with MAb 58B1. We have shown, however, that extracellular microdomain labeling persists for at least 1 day after we remove cholesterol-enriched macrophages from culture plates with repeated freeze-thaw cycles. This suggests that extracellular microdomains deposited by macrophages can be mobilized by the macrophages either by being taken up by the macrophages or possibly solubilized by a macrophage-derived mediator of cholesterol efflux. In regards to the latter, human monocyte-derived macrophages produce nascent apolipoprotein E-discoidal HDL particles that are capable of mobilizing cholesterol without addition of exogenous cholesterol acceptors (33, 34). Thus, while deposition of microdomains onto the extracellular matrix may depend on actin microfilaments, it is possible that the reuptake or solubilization of extracellular cholesterol-rich microdomains can occur independently of actin microfilament function. This proposed mechanism would account for the lack of extracellular microdomain labeling observed in the cytochalasin D experiment (i.e., cytochalasin D blocks deposition) as well as the persistence of extracellular microdomain labeling seen in the freeze-thaw experiment (i.e., macrophages are required to mobilize the deposited cholesterol).

Src family tyrosine kinases functioned in the macrophage deposition of unesterified cholesterol-rich microdomains into the extracellular matrix. Cultures incubated with AcLDL in the presence of the Src family tyrosine kinase inhibitor, SU6656, showed increased unesterified cholesterol-rich microdomain labeling on cell surfaces but no labeling in the extracellular matrix when compared with cultures incubated with AcLDL alone. Nevertheless, macrophage cultures incubated with AcLDL in the presence of SU6656 accumulated the same quantity of total cholesterol as cultures incubated with AcLDL alone. These findings suggest that unesterified cholesterol-rich microdomain deposition occurs through a two-step process in which macrophages first accumulate unesterified cholesterol in the form of cell surface microdomains through a mechanism involving actin microfilaments. These cell surface microdomains are subsequently deposited onto the extracellular matrix through a mechanism requiring Src

family kinase activity. Src family kinases are known to be involved in the regulation of the actin cytoskeleton (25–27), and thus, the effects of SU6656 on cholesterol processing may be partially explained by disruption of actin function. Indeed, cholesterol-enriched macrophages that were treated with SU6656 and those that were treated with cytochalasin D develop the same stellate morphology that distinguishes them from cholesterol-enriched macrophages that do not receive treatment. However, treatment with SU6656 and treatment with cytochalasin D showed different effects on development of cholesterol-rich microdomains. Plasma membrane cholesterol-rich domains developed with SU6656 but were absent with cytochalasin D treatment. This suggests that SU6656 and cytochalasin D have different effects on cholesterol processing. It is possible that inhibition of Src family kinase activity does not affect the actin cytoskeleton by causing microfilament depolymerization or that either SU6656 or cytochalasin D have other properties besides their effects on the actin cytoskeleton. For example, Src family kinases are known to be involved in the regulation of other cytoskeletal structures, including microtubules (35, 36). We investigated the effect of disrupting tubulin polymerization using nocodazole, however, and found that it did not eliminate extracellular labeling or increase cell surface labeling of unesterified cholesterol-rich microdomains when cultures were stained with MAb 58B1. The specific mechanism by which Src family kinases regulate cholesterol processing in M-CSF-differentiated macrophages therefore remains uncertain.


In addition to studying the processes behind the generation of extracellular cholesterol-rich microdomains, we also evaluated the potential for these microdomains to function in reverse cholesterol transport. Our results show that the cholesterol acceptors, apoA-I and HDL, can function in mobilization of unesterified cholesterol-rich microdomains from the extracellular matrix. Cholesterol quantification assays revealed that treatment with apoA-I or HDL resulted in a significant reduction in the amount of unesterified but not esterified cholesterol in cholesterol-enriched cultures. Cholesterol within macrophages has been shown to shift between esterified and unesterified forms due to its continuous hydrolysis and reesterification (37). Thus, cholesterol removal from cells might be expected to reduce the cellular content of both esterified and unesterified cholesterol. The extracellular cholesterol microdomains identified using MAb 58B1, however, may not undergo continuous hydrolysis and reesterification. The ready mobilization of these extracellular deposits could therefore account for the isolated reduction in unesterified cholesterol content in cholesterol-enriched cultures treated with a cholesterol acceptor.

We also found that apoA-I-mediated removal of extracellular unesterified cholesterol requires the presence of cells, and in particular, the function of ABCA1 as suggested by glyburide inhibition of cholesterol removal. This result is consistent with previous studies regarding the mechanism of apoA-I-mediated removal of unesterified

cholesterol from cell surfaces that have shown that ABCA1 functions in the phospholipidation of apoA-I, transforming it into nascent HDL that can then remove cholesterol (32). In agreement with this proposed mechanism, HDL was capable of removing extracellular unesterified cholesterol-rich microdomains even in the absence of cells and therefore without the need for phospholipidation by ABCA1, presumably because HDL is already rich in phospholipid.

Burgess et al. (38) have established the existence of phospholipid-containing sites in the macrophage extracellular matrix that are capable of binding apoA-I. These sites were found to promote cellular cholesterol efflux through an ABCA1-dependent mechanism. Our cholesterol-rich extracellular sites do not appear to be identical with these phospholipid-rich extracellular sites. The extracellular phospholipid-rich sites underlie cultured macrophages, while the extracellular cholesterol-rich sites we describe occur in the extracellular matrix between macrophages. However, further study is required to determine the origins and possible functional relationships of these extracellular cholesterol and phospholipid lipid-containing sites.

Because unesterified cholesterol-rich cell surface microdomains can function in reverse cholesterol transport, it remains curious as to what purpose the deposition of these microdomains onto the extracellular matrix serves. Our finding that extracellular microdomains can function in reverse cholesterol transport in the absence of cells suggests a potential explanation. Excessive accumulation of cholesterol has been shown to be toxic to macrophages in culture (8, 9), consistent with the histological observation that lipid-laden areas of atherosclerotic plaques are often relatively acellular. It is therefore possible that cholesterol-enriched macrophages process unesterified cholesterol into an extracellular form to prevent buildup of toxic levels of cholesterol within the macrophage that under certain conditions can lead to macrophage apoptosis. Our other finding that extracellular unesterified cholesterol-rich microdomains are found within atherosclerotic lesions supports the idea that the reverse cholesterol transport system may not function efficiently within atherosclerotic plaques.

In summary, we have shown that cholesterol-enriched human monocyte-derived macrophages in culture produce unesterified cholesterol-rich cell surface microdomains. These microdomains transfer to the extracellular matrix through a mechanism regulated by Src family kinases. Both cell surface unesterified cholesterol-rich microdomains and extracellular unesterified cholesterol-rich microdomains are capable of removal by the cholesterol acceptors, apoA-I and HDL, and may therefore function in reverse cholesterol transport. ABCA1-generated cholesterol-containing microparticles released into the medium by cultured cells have been described (33, 39, 40). In future studies, it will be of interest to learn whether ABC family transporters function in the generation of the extracellular microparticles showing cholesterol-rich microdomains reported here. 

The authors thank the Department of Transfusion Medicine, Clinical Center, National Institutes of Health, for providing elutriated monocytes, Qing Xu and Janet Chang for technical assistance, and Dr. Neil J. Freedman for critical reading of the manuscript.

REFERENCES

1. Kruth, H. S. 2001. Macrophage foam cells and atherosclerosis. *Front. Biosci.* **6**: D429–D455.
2. Gerrity, R. G. 1981. The role of the monocyte in atherogenesis: I. Transition of blood-borne monocytes into foam cells in fatty lesions. *Am. J. Pathol.* **103**: 181–190.
3. Gerrity, R. G. 1981. The role of the monocyte in atherogenesis: II. Migration of foam cells from atherosclerotic lesions. *Am. J. Pathol.* **103**: 191–200.
4. Cuchel, M., and D. J. Rader. 2006. Macrophage reverse cholesterol transport: key to the regression of atherosclerosis? *Circulation.* **113**: 2548–2555.
5. Stary, H. C., A. B. Chandler, S. Glagov, J. R. Guyton, W. Insull, Jr., M. E. Rosenfeld, S. A. Schaffer, C. J. Schwartz, W. D. Wagner, and R. W. Wissler. 1994. A definition of initial, fatty streak, and intermediate lesions of atherosclerosis. A report from the Committee on Vascular Lesions of the Council on Arteriosclerosis, American Heart Association. *Circulation.* **89**: 2462–2478.
6. Daugherty, A., D. L. Rateri, and H. Lu. 2008. As macrophages indulge, atherosclerotic lesions bulge. *Circ. Res.* **102**: 1445–1447.
7. Kruth, H. S. 1984. Localization of unesterified cholesterol in human atherosclerotic lesions. Demonstration of filipin-positive, oil-red-O-negative particles. *Am. J. Pathol.* **114**: 201–208.
8. Yao, P. M., and I. Tabas. 2000. Free cholesterol loading of macrophages induces apoptosis involving the fas pathway. *J. Biol. Chem.* **275**: 23807–23813.
9. Kellner-Weibel, G., Y. J. Geng, and G. H. Rothblat. 1999. Cytotoxic cholesterol is generated by the hydrolysis of cytoplasmic cholesteryl ester and transported to the plasma membrane. *Atherosclerosis.* **146**: 309–319.
10. Hegyi, L., J. N. Skepper, N. R. Cary, and M. J. Mitchinson. 1996. Foam cell apoptosis and the development of the lipid core of human atherosclerosis. *J. Pathol.* **180**: 423–429.
11. Chao, F. F., L. M. Amende, E. J. Blanchette-Mackie, S. I. Skarlatos, W. Gamble, J. H. Resau, W. T. Mergner, and H. S. Kruth. 1988. Unesterified cholesterol-rich lipid particles in atherosclerotic lesions of human and rabbit aortas. *Am. J. Pathol.* **131**: 73–83.
12. Chao, F. F., E. J. Blanchette-Mackie, B. F. Dickens, W. Gamble, and H. S. Kruth. 1994. Development of unesterified cholesterol-rich lipid particles in atherosclerotic lesions of WHHL and cholesterol-fed NZW rabbits. *J. Lipid Res.* **35**: 71–83.
13. Norman, A. W., R. A. Demel, B. de Kruffy, and L. L. van Deenen. 1972. Studies on the biological properties of polyene antibiotics. Evidence for the direct interaction of filipin with cholesterol. *J. Biol. Chem.* **247**: 1918–1929.
14. Perl-Treves, D., N. Kessler, D. Izhaky, and L. Addadi. 1996. Monoclonal antibody recognition of cholesterol monohydrate crystal faces. *Chem. Biol.* **3**: 567–577.
15. Kruth, H. S., I. Ifrim, J. Chang, L. Addadi, D. Perl-Treves, and W. Y. Zhang. 2001. Monoclonal antibody detection of plasma membrane cholesterol microdomains responsive to cholesterol trafficking. *J. Lipid Res.* **42**: 1492–1500.
16. Waldo, S. W., Y. Li, C. Buono, B. Zhao, E. M. Billings, J. Chang, and H. S. Kruth. 2008. Heterogeneity of human macrophages in culture and in atherosclerotic plaques. *Am. J. Pathol.* **172**: 1112–1126.
17. Kruth, H. S., S. I. Skarlatos, K. Lilly, J. Chang, and I. Ifrim. 1995. Sequestration of acetylated LDL and cholesterol crystals by human monocyte-derived macrophages. *J. Cell Biol.* **129**: 133–145.
18. Hashimoto, S., M. Yamada, K. Motoyoshi, and K. S. Akagawa. 1997. Enhancement of macrophage colony-stimulating factor-induced growth and differentiation of human monocytes by interleukin-10. *Blood.* **89**: 315–321.
19. Folch, J., M. Lees, and G. H. Sloane Stanley. 1957. A simple method for the isolation and purification of total lipides from animal tissues. *J. Biol. Chem.* **226**: 497–509.
20. Gamble, W., M. Vaughan, H. S. Kruth, and J. Avigan. 1978. Procedure for determination of free and total cholesterol in mi-

- cro- or nanogram amounts suitable for studies with cultured cells. *J. Lipid Res.* **19**: 1068–1070.
21. Lowry, O. H., N. J. Rosebrough, A. L. Farr, and R. J. Randall. 1951. Protein measurement with the Folin phenol reagent. *J. Biol. Chem.* **193**: 265–275.
 22. Smith, E. B., P. H. Evans, and M. D. Downham. 1967. Lipid in the aortic intima. The correlation of morphological and chemical characteristics. *J. Atheroscler. Res.* **7**: 171–186.
 23. Cooper, J. A. 1987. Effects of cytochalasin and phalloidin on actin. *J. Cell Biol.* **105**: 1473–1478.
 24. Swanson, J., A. Bushnell, and S. C. Silverstein. 1987. Tubular lysosome morphology and distribution within macrophages depend on the integrity of cytoplasmic microtubules. *Proc. Natl. Acad. Sci. USA.* **84**: 1921–1925.
 25. Angers-Loustau, A., R. Hering, T. E. Werbowetski, D. R. Kaplan, and R. F. Del Maestro. 2004. SRC regulates actin dynamics and invasion of malignant glial cells in three dimensions. *Mol. Cancer Res.* **2**: 595–605.
 26. Destaing, O., A. Sanjay, C. Itzstein, W. C. Horne, D. Toomre, P. De Camilli, and R. Baron. 2008. The tyrosine kinase activity of c-Src regulates actin dynamics and organization of podosomes in osteoclasts. *Mol. Biol. Cell.* **19**: 394–404.
 27. Kilarski, W. W., N. Jura, and P. Gerwins. 2003. Inactivation of Src family kinases inhibits angiogenesis in vivo: implications for a mechanism involving organization of the actin cytoskeleton. *Exp. Cell Res.* **291**: 70–82.
 28. Smolinska, M. J., N. J. Horwood, T. H. Page, T. Smallie, and B. M. Foxwell. 2008. Chemical inhibition of Src family kinases affects major LPS-activated pathways in primary human macrophages. *Mol. Immunol.* **45**: 990–1000.
 29. Blake, R. A., M. A. Broome, X. Liu, J. Wu, M. Gishizky, L. Sun, and S. A. Courtneidge. 2000. SU6656, a selective src family kinase inhibitor, used to probe growth factor signaling. *Mol. Cell. Biol.* **20**: 9018–9027.
 30. Marcel, Y. L., M. Ouimet, and M. D. Wang. 2008. Regulation of cholesterol efflux from macrophages. *Curr. Opin. Lipidol.* **19**: 455–461.
 31. Tall, A. R., L. Yvan-Charvet, N. Terasaka, T. Pagler, and N. Wang. 2008. HDL, ABC transporters, and cholesterol efflux: implications for the treatment of atherosclerosis. *Cell Metab.* **7**: 365–375.
 32. Fielding, P. E., K. Nagao, H. Hakamata, G. Chimini, and C. J. Fielding. 2000. A two-step mechanism for free cholesterol and phospholipid efflux from human vascular cells to apolipoprotein A-I. *Biochemistry.* **39**: 14113–14120.
 33. Kruth, H. S., S. I. Skarlatos, P. M. Gaynor, and W. Gamble. 1994. Production of cholesterol-enriched nascent high density lipoproteins by human monocyte-derived macrophages is a mechanism that contributes to macrophage cholesterol efflux. *J. Biol. Chem.* **269**: 24511–24518.
 34. Zhang, W. Y., P. M. Gaynor, and H. S. Kruth. 1996. Apolipoprotein E produced by human monocyte-derived macrophages mediates cholesterol efflux that occurs in the absence of added cholesterol acceptors. *J. Biol. Chem.* **271**: 28641–28646.
 35. Sulimenko, V., E. Draberova, T. Sulimenko, L. Macurek, V. Richterova, and P. Draber. 2006. Regulation of microtubule formation in activated mast cells by complexes of gamma-tubulin with Fyn and Syk kinases. *J. Immunol.* **176**: 7243–7253.
 36. Talmor-Cohen, A., R. Tomashov-Matar, W. B. Tsai, W. H. Kinsey, and R. Shalgi. 2004. Fyn kinase-tubulin interaction during meiosis of rat eggs. *Reproduction.* **128**: 387–393.
 37. Brown, M. S., Y. K. Ho, and J. L. Goldstein. 1980. The cholesterol ester cycle in macrophage foam cells. Continual hydrolysis and re-esterification of cytoplasmic cholesterol esters. *J. Biol. Chem.* **255**: 9344–9352.
 38. Burgess, J. W., R. S. Kiss, H. Zheng, S. Zachariah, and Y. L. Marcel. 2002. Trypsin-sensitive and lipid-containing sites of the macrophage extracellular matrix bind apolipoprotein A-I and participate in ABCA1-dependent cholesterol efflux. *J. Biol. Chem.* **277**: 31318–31326.
 39. Liu, L., A. E. Bortnick, M. Nickel, P. Dhanasekaran, P. V. Subbaiah, S. Lund-Katz, G. H. Rothblat, and M. C. Phillips. 2003. Effects of apolipoprotein A-I on ATP-binding cassette transporter A1-mediated efflux of macrophage phospholipid and cholesterol: formation of nascent high density lipoprotein particles. *J. Biol. Chem.* **278**: 42976–42984.
 40. Nandi, S., L. Ma, M. Denis, J. Karwatsky, Z. Li, X. C. Jiang, and X. Zha. 2009. ABCA1-mediated cholesterol efflux generates microparticles in addition to HDL through processes governed by membrane rigidity. *J. Lipid Res.* **50**: 456–466.